

# Dynamic viscosity of macroscopic suspensions of bimodal sized solid spheres

Philippe Gondret<sup>a)</sup>

*Laboratoire Fluides, Automatique et Systèmes Thermiques-URA 871 du CNRS, Universités Paris-Sud et Pierre et Marie Curie, Batiment 502, Campus Universitaire, F-91405 Orsay Cedex, France*

Luc Petit

*Laboratoire de Physique de la Matière Condensée-UMR 6622 du CNRS, Université de Nice, Parc Valrose, F-06108 Nice Cedex 2, France*

(Received 4 February 1997; final revision received 8 August 1997)

## Synopsis

In this paper, we present experimental measurements for the dynamic viscosity of macroscopic (non-Brownian and noncolloidal) suspensions of bimodal sized spheres when submitted to an oscillating plane Couette flow. The measured viscosity is what we call the dynamic viscosity at finite frequency. Concerning the viscosity of such systems, numerous experimental studies have been done under steady flow conditions, i.e., at zero frequency, but few studies concern the dynamic case. Our measurements have been performed for different values of the three relevant parameters, namely the size ratio  $\lambda$ , the fraction  $\xi$  of small spheres to total solids, and the total solid volume fraction  $\Phi$ . Our results show a viscosity reduction upon mixing, which increases as the total solid volume fraction  $\Phi$  is increased. We analyze our results by a model that takes into account the volume fraction  $\Phi$  and the maximum volume fraction  $\Phi_m$ , which depends on the two parameters  $\lambda$  and  $\xi$ . On the other hand, we compare our experimental results with recent numerical simulations performed by Chang and Powell [J. Fluid Mech. **253**, 1–25 (1993); Phys. Fluids **6**, 1628–1636 (1994)] by Stokesian dynamics, and Monte Carlo method, which lead, respectively, to viscosity at zero and infinite frequency. Our experimental results lie between these two different simulation results. © 1997 The Society of Rheology. [S0148-6055(97)00906-1]

## I. INTRODUCTION

The rheological properties of suspensions made of particles that are bi- or polydisperse in size are important to know for a better understanding of their flow behavior. In numerous materials, the functional performance is linked to the total amount of solid, such as in solid rocket propellants [Miller *et al.* (1991)] or dental pastes [Cheng *et al.* (1990)]. In such cases where high volume loadings are desired, the concomitant high viscosity is usually not favorable from a processing standpoint. However, high solid loadings can be attained with a small increase in viscosity using suspensions having a distribution of particle sizes rather than particles of similar sizes [Lee (1970)]. The study of polydisperse suspensions, and more fundamentally, of bidisperse suspensions is, thus,

---

<sup>a)</sup>Corresponding author.

of considerable interest, and several works either experimental, numerical, or theoretical have been done in the past.

In the case of colloidal suspensions, there are the works of Parkinson *et al.* (1970), of Woutersen and De Kruif (1993), and of D'Haene and Mewis (1994). However, in this paper we will focus on what we call the macroscopic suspensions, in which Brownian effects and surface forces can be neglected when compared to hydrodynamic forces.

In the case of bidisperse macroscopic suspensions of solid spheres, several experimental studies measuring the viscosity of such systems have been performed using different types of viscometers but most of these studies deal with steady flows, i.e., at zero frequency. Indeed, Sweeny and Geckler (1954), followed by Eveson (1959), Hoffman (1992), Shapiro and Probst (1992), Probst *et al.* (1994), and Chang and Powell (1994b) have used a concentric cylinder or a cone-plate viscometer; in the induced shear flows, the steady-shear viscosity is calculated by measuring the angular velocity of the moving part and the shear stress acting on it. On the other hand, Chong *et al.* (1971) and later Storms *et al.* (1990) have used an orifice viscometer in which suspensions are driven through an abrupt contraction; the viscosity is here calculated by measuring the pressure drop and the flow rate. At last, Goto and Kuno (1982, 1984) have used a capillary viscometer with which they have been able both to measure the steady-shear viscosity and to visualize the particles inside the tube. All these experimental results show the same general trend: a viscosity reduction upon mixing, which increases with increasing size ratio. Note that when the particle size ratio is sufficiently large (more than roughly 10), the small particles can be viewed as a continuous fluid with respect to large ones [Farris (1968), Sengun and Probst (1989)]: beyond this "critical" size ratio, the small spheres can easily migrate through the interstices of the large spheres.

By contrast, very few experiments have been performed in the case of dynamic shear flows, i.e., at nonzero frequency. Concerning the colloidal suspensions, Kim and Luckham (1993) have measured the dynamic viscosity of bidisperse polystyrene latex particles ( $d = 0.2$  and  $1.4 \mu\text{m}$ ) over the frequency range  $10^{-2}$ –10 Hz with a concentric cylinder rheometer used in the oscillatory shear mode. Concerning the macroscopic suspensions, Poslinski *et al.* (1988) have measured the dynamic viscosity of bidisperse suspensions of glass spheres ( $d = 15$  and  $80 \mu\text{m}$ ) in a high viscous polymer (polybutene,  $\eta = 25 \text{ Pa s}$ ) with a parallel-plate viscometer. However, these last authors have not reported the dynamic viscosity at a precise frequency but only around 10 Hz. Indeed, they average their dynamic viscosity measurements over the frequency range 1.6–16 Hz.

Beside all these experimental studies, numerical simulations have been performed just recently. Chang and Powell (1993, 1994a) have used Stokesian dynamics to calculate the viscosity for a monolayer of a suspension of bimodally distributed spherical particles located in the plane of shear. These two-dimensional (2D) simulations rather than full three-dimensional (3D) ones minimize computation costs while preserving the essential physics (both the far-field many-body interactions and the near-field lubrication forces are explicitly included). In dynamic simulations [Chang and Powell (1993)], the suspension undergoes an imposed shear flow and the positions of the particles evolve and are followed at each time step: steady state occurs after a large number of time steps and can lead to the formation of clusters. The calculated viscosity corresponds to the steady viscosity at zero frequency and large rate of strain. In the Monte Carlo technique [Chang and Powell (1994a)], the microstructure does not evolve in time as occurs in a dynamic simulation: several samples are generated and the viscosity is calculated for each sample and averaged over all the samples. The calculated viscosity corresponds here to the dynamic viscosity at a high frequency and small rate of strain. These two different techniques of simulations both give a viscosity reduction upon mixing, which increases

with the size ratio. However, dynamic simulation is found to yield higher viscosities as compared with the results of the Monte Carlo simulations.

At last, very few theoretical works deal with this problem. Only recently, exact numerical calculations have been made by Wagner and Woutersen (1994) for the dilute limiting, zero shear viscosity of bimodal suspension of hard spheres: the hydrodynamic functions have been calculated using previous theoretical results [Jeffrey (1992)] for the hydrodynamic resistivities between pairs of hard spherical particles of different radii. The results show that both the hydrodynamic and Brownian contributions to the Huggins coefficient (namely, the second-order coefficient of the viscosity when expanded in terms of powers of the total solid volume fraction) exhibit a minimum, which is symmetric in mixing volume fraction and which deepens with increasing size ratio. The reduction of viscosity upon mixing is seen by the authors to be a result of near-field hydrodynamic shielding of asymmetric particle pairs.

We have performed extensive experiments on suspensions of solid spherical particles in order to study the influence of the bimodal distribution of the particle size on the viscosity of such systems. Our investigation concerns the measurement of the dynamic viscosity, i.e., the viscosity in the case of an oscillating shear flow at finite frequency. The measurements have been made a short time after the application of the flow in order to obtain the viscosity before the beginning of any possible ordering of the suspension under the action of the oscillating flow. This effect, which has been previously observed and studied, is reported elsewhere [Gondret and Petit (1993, 1996)].

In the following paragraph, we give the features of the suspensions we have used and the experimental conditions for the viscosity measurements. In a subsequent paragraph, we present the results we obtained and compare them to other experimental data and recent numerical simulations. Furthermore, we propose a model based on the influence of the size distribution of the particles on their packing fraction, and so, on the viscosity.

## II. EXPERIMENT

### A. Materials

The suspension we have studied are made of glass spheres of diameter in the range 45–450  $\mu\text{m}$ , embedded in a silicon oil (polydimethylsiloxane) of viscosity 5 Pa s. Each particle size is obtained by sieving mechanically the particles. For each of the corresponding size distributions, the ratio  $\sigma_d/\bar{d}$  is around 10%, where  $\bar{d}$  is the mean diameter and  $\sigma_d$  the standard deviation.

The particles of the two sizes, with the diameter  $d_S = 45 \mu\text{m}$  for the small ones and  $d_L = \lambda d_S$  for the large ones ( $\lambda = 2\text{--}10$  is the size ratio), are mixed together with a given volume of each size leading to a known value of the fraction  $\xi$  of small spheres to total solids [ $\xi = V_S/(V_S+V_L)$ ,  $0 < \xi < 1$ ]. The particles are then embedded in a given volume  $V_f$  of fluid, leading to a known value of the total solid volume fraction  $\Phi = (V_S+V_L)/(V_S+V_L+V_f)$ . At last, the fluid–particle mixture is stirred manually to homogenize it and is then kept at rest to remove air bubble.

### B. Viscosity measurement

The suspension is submitted to an oscillating plane shear flow between two parallel glass plates separated by a small gap. The lower plate is fixed and the upper one is moving alternatively at a given frequency  $f$  ( $f = 200$  Hz for the results reported in this paper). The particle Reynolds number is low ( $\text{Re} \approx 10^{-2}$ ), meaning that inertial forces are much smaller than viscous forces. Owing to the large sizes of the particles (much larger than the micrometer), the Péclet number is very high ( $\text{Pe} \approx 10^{11}$ ), meaning that

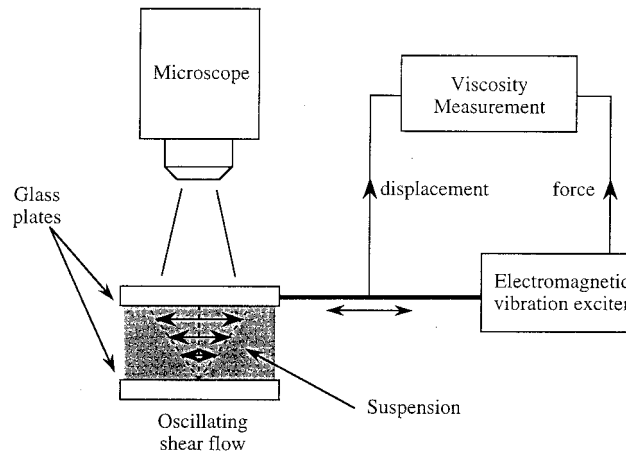


**FIG. 1.** Sketch of the experimental setup. The suspension is placed between two parallel glass plates allowing microscopic visualization. The upper plate oscillates under the action of an electromagnetic vibrator while the lower one is at rest. The viscosity of the suspension is measured from the phase shift between the driving force and the induced displacement of the upper plate.

hydrodynamic interactions between the particles dominate surface forces and Brownian effects. Figure 1 shows a schematic view of the experimental setup and flow geometry. Viscosity measurements are performed by measuring the phase shift between the strength applied to the moving plate and its displacement. This phase shift is directly related to the dynamic viscosity  $\eta$  of the suspension lying between the plates. The strain amplitude is small ( $\gamma_0 \approx 0.1$ ) and we have checked that we were in the linear region. Indeed, the oscillating character of the applied flow allowed us to check easily that the response remained sinusoidal. More details about the setup and the method of viscosity measurements can be found in Gondret and Petit (1996).

The visualization of the suspension during the flow is achieved by means of an optical microscope with a lighting synchronized at the frequency of the shear flow. This allows us to observe particle migration [Petit and Gondret (1993)] and a possible shear-induced ordering [Gondret and Petit (1993)]. Note that all the results presented in this paper correspond to measurements made just after starting the shear (typically a few seconds later) in order to avoid any structure formation we can observe after a long time of shearing [Gondret and Petit (1993, 1996)].

To sum up, the dynamic viscosity measurements presented in this paper correspond to the viscosity of disordered suspensions of non-Brownian hard spheres at finite frequency and low strain amplitude.

### III. RESULTS AND DISCUSSION

#### A. Viscosity and maximum solid fraction

The results we obtain for the viscosity measurement of monodisperse suspensions with the experimental conditions described in the previous section are presented in Fig. 2 (open circles). A monotonic increase of the viscosity as the volume fraction  $\Phi$  is increased can be seen, with a strong increase as  $\Phi$  approaches values around 0.6. This is a classical behavior.

A standard way to model the viscosity of non-Brownian suspension of hard spheres is to use an effective medium approach [Van de Ven (1989)]. This leads to a relation

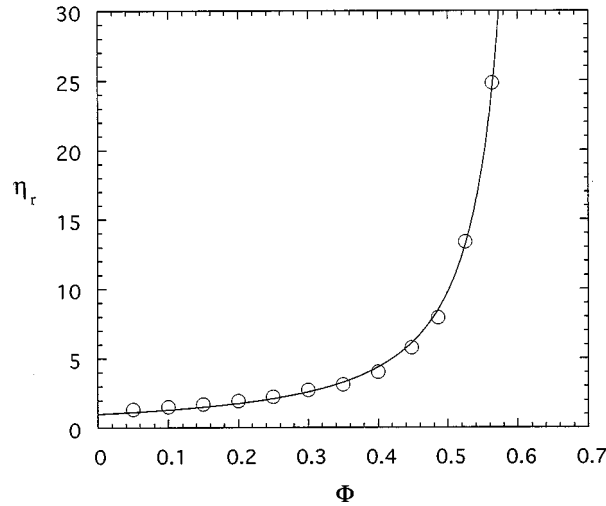


**FIG. 2.** Relative viscosity,  $\eta_r$ , of suspensions of solid spheres as a function of the solid volume fraction  $\Phi$ . (○): Viscosity measurements for monodisperse suspensions of glass spheres ( $45 \mu\text{m}$  in diameter) for the oscillating frequency  $f = 200 \text{ Hz}$ . (—): Values given by the effective medium model [Eq. (1)] with the maximum volume fraction  $\Phi_m = 0.64$ . This value of  $\Phi_m$  was obtained from the best fit of the experimental data.

between the relative viscosity, defined as the ratio of the viscosity of the suspension to the viscosity of the suspending fluid, and the solid volume fraction, which is usually termed the Krieger–Dougherty relation and which is of the following kind:

$$\eta_r = \left(1 - \frac{\Phi}{\Phi_m}\right)^{-\alpha}, \tag{1}$$

where  $\Phi_m$  is the maximum solid volume fraction of the suspension and  $\alpha$  an exponent that characterizes the divergence when  $\Phi$  approaches  $\Phi_m$ . The value of  $\alpha$  is usually between 1 and 2, depending on the interactions between the particle [Ball and Richmond (1980), De Kruij *et al.* (1985), Brady (1993)]. The best fit of our experimental data (solid line in Fig. 2) leads to the values  $\alpha = 1.5 \pm 0.1$  and  $\Phi_m = 0.64 \pm 0.01$  [Gondret and Petit (1995)]. This value of  $\Phi_m$  is the value of the packing fraction  $c_0$  found for random close packings of dry hard spheres, both experimentally, numerically, and theoretically [Scott and Kilgour (1969), Nolan and Kavanagh (1992), Sadoc (1981)]. This is not surprising since our suspensions are disordered. If the suspensions are ordered by the flow, the value of  $\Phi_m$  can be larger [De Kruij *et al.* (1985), Gondret and Petit (1995)]. Note that there is no *a priori* reason for the maximum solid fraction of a disordered suspension of spheres to be strictly equal to the random close packing fraction of dry hard spheres. Indeed, Shapiro and Probst (1992) found the factor 1.19 between the two and named it the ‘‘filler dilatancy factor’’ [Probst *et al.* (1994)]. However, this is the case for our monodisperse suspensions and we will assume that it stands for the bidisperse suspensions. It is reasonable as the filler dilatancy factor of 1.19 found by Probst *et al.* (1994) seems not to change with the size ratio  $\lambda$  and the composition  $\xi$ . In the bidisperse case, the random close-packing fraction  $c$  depends on the two parameters  $\lambda$  and  $\xi$ , and in the following, we will model the viscosity of bidisperse suspensions by the relation

$$\eta_r = \left(1 - \frac{\Phi}{\Phi_m(\lambda, \xi)}\right)^{-1.5} \quad \text{with } \Phi_m(\lambda, \xi) = c(\lambda, \xi), \quad (2)$$

where  $c(\lambda, \xi)$  is calculated from the model of Ouchiyama and Tanaka (1981) as suggested by Gupta and Seshadri (1986). This model is presented below and compared to experimental and simulation results.

## B. Packing fraction

To our knowledge, three main different models exist for predicting the packing fraction of bidisperse packings of hard spheres as a function of the size ratio  $\lambda$  and of the fraction  $\xi$  of small spheres: the ones of Ben Aim and Le Goff (1967), of Dodds (1980), and of Ouchiyama and Tanaka (1981). In all these models, the random dense packing fraction of monodisperse spheres  $c_0$  is a free parameter for which we choose the value  $c_0 = 0.64$ .

The simplest model, only valid for spheres of two very different sizes, i.e., for  $\lambda \rightarrow \infty$ , leads to the following relations:

$$c(\lambda, \xi) = \frac{c_0}{1 - \xi} \quad (\xi \rightarrow 0), \quad (3)$$

$$c(\lambda, \xi) = \frac{c_0}{1 - (1 - \xi)(1 - c_0)} \quad (\xi \rightarrow 1). \quad (4)$$

The first relation is obtained when considering that few small particles are in the interstices of a monodisperse packing of large particles. For the second relation, few large particles are dispersed into a monodisperse packing of small particles. At the point where the two functions cross each other, the packing fraction is maximum:  $c_{\max} = c_0(2 - c_0)$  at  $\xi_{\max} = (1 - c_0)/(2 - c_0)$ . With the value  $c_0 = 0.64$  for the monodisperse packing fraction, it leads to  $c_{\max} = 0.870$  and  $\xi_{\max} = 0.265$ . This simple model gives the limiting curve under which must be the packing fraction of all bidisperse random packings.

Ben Aim and Le Goff (1967) take into account the linear perturbation for the packing fraction near a large sphere embedded in a packing of small spheres. Their model is, therefore, only correct for a large size ratio ( $\lambda > 10$ ).

The model of Dodds consists in first calculating the solid fraction over a tetrahedron made of four spheres in contact. Depending on the sizes of the four spheres, the tetrahedron is not the same and neither its solid fraction. The packing fraction is then simply calculated considering the fraction of each tetrahedron in the packing, which depends on the fraction  $\xi$  of the small spheres. The main problem is that the three-dimensional space cannot be filled with an assembly of tetrahedra in contact.

The model we used is the one proposed by Ouchiyama and Tanaka (1981). It consists of replacing the real packing of spheres by a homogenized one in the following way (Fig. 3): each sphere (of diameter  $d$ ) of the original packing is considered successively as the ‘reference’ sphere (central dark grey sphere in Fig. 3). Its neighbors in contact (of diameter  $d_i$ ) are all replaced by the same number of spheres of the same diameter equal to the mean diameter  $\bar{d}$  of the packing. The packing fraction is then calculated over the spherical cell of diameter  $d + \bar{d}$  (dotted circle in Fig. 3). Its expression in terms of the two parameters  $\lambda$  and  $\xi$  is

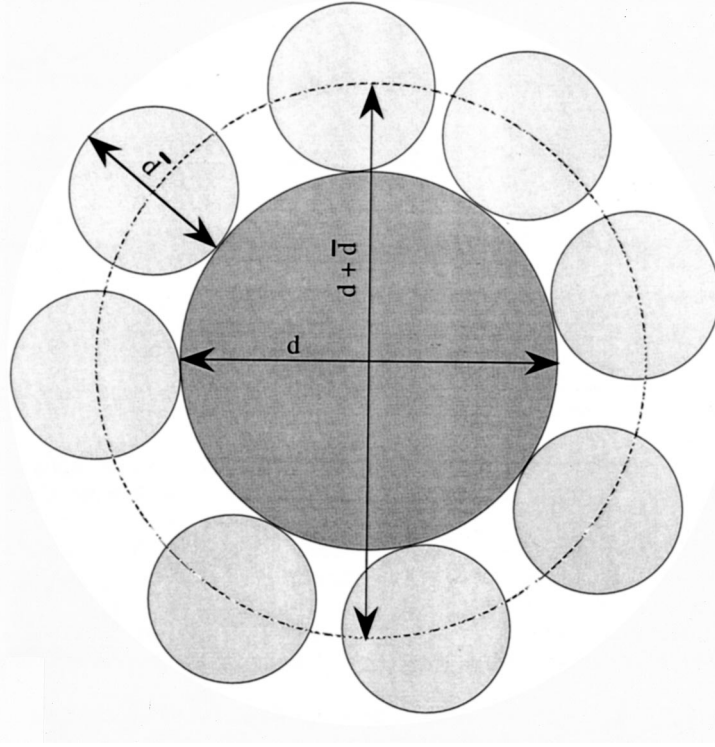


**FIG. 3.** Basic cell of the model of Ouchiyaama and Tanaka (1981) for the calculation of the packing fraction of the bidisperse packing of spheres. In this cell (dotted circle) the real packing is replaced by a homogenized one. The neighboring spheres of different diameter  $d_i$  in contact with a central reference sphere of diameter  $d$  in the real packing (in dark grey) are replaced by the same number of spheres of all the same diameter equal to the mean diameter  $\bar{d}$  of the packing. The packing fraction can then be easily calculated in the spherical cell of diameter  $d + \bar{d}$  (dotted circle).

$$c(\lambda, \xi) = \frac{N_S \tilde{d}_S + N_L \tilde{d}_L}{(N_S/\Gamma)(\tilde{d}_S + 1)^3 + N_L\{(\tilde{d}_L - 1)^3 + 1/\Gamma[(\tilde{d}_L + 1)^3 - (\tilde{d}_L - 1)^3]\}}, \quad (5)$$

where  $N_S$  and  $N_L$  are the number fractions of small and large spheres, respectively,  $\tilde{d}_S$  and  $\tilde{d}_L$  the diameters of the small and large particles normalized by the mean diameter  $\bar{d}$ , and  $1/\Gamma$  can be seen as the fraction of the spherical shell allocated to the reference sphere. Each of these parameters depends on  $\lambda$  and  $\xi$  as follows:

$$N_S = \frac{\xi \lambda^3}{\xi \lambda^3 + (1 - \xi)} \quad \text{and} \quad N_L = \frac{1 - \xi}{\xi \lambda^3} N_S, \quad (6)$$

$$\tilde{d}_S = \frac{d_S}{\bar{d}} = \frac{\xi \lambda^3 + (1 - \xi)}{\xi \lambda^3 + (1 - \xi) \lambda} \quad \text{and} \quad \tilde{d}_L = \frac{d_L}{\bar{d}} = \lambda \tilde{d}_S, \quad (7)$$

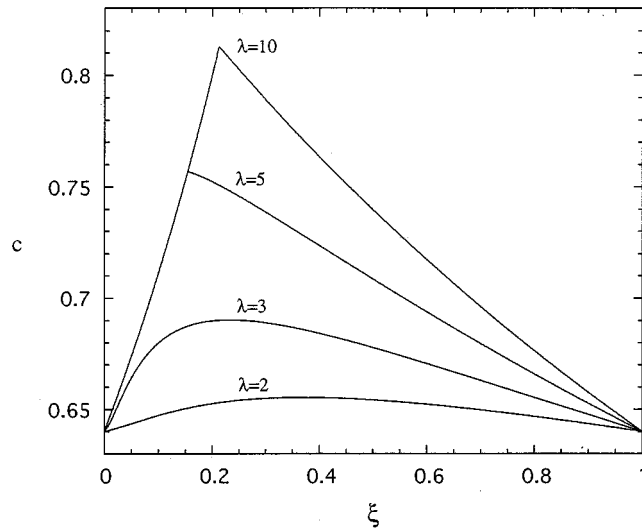


**FIG. 4.** Packing fraction  $c$  of packings of bidisperse spheres of size ratio  $\lambda$  as a function of the proportion of smaller spheres  $\xi$ , calculated from the model of Ouchiyama and Tanaka (1981).

$$\Gamma = 1 + \frac{4}{13}(8c_0 - 1) \frac{N_S(\tilde{d}_S + 1)^2 \left(1 - \frac{3}{8} \frac{1}{\tilde{d}_S + 1}\right) + N_L(\tilde{d}_L + 1)^2 \left(1 - \frac{3}{8} \frac{1}{\tilde{d}_L + 1}\right)}{N_S \tilde{d}_S^3 + N_L[\tilde{d}_L^3 - (\tilde{d}_L - 1)^3]} \quad (8)$$

The results given by this model are presented in Fig. 4, where the packing fraction  $c$  is plotted as a function of the fraction  $\xi$  of small spheres for different value of the size ratio  $\lambda$ . The general feature is an increase in the packing fraction  $c$  as the size ratio  $\lambda$  is increased, with a maximum of  $c$  even more pronounced as  $\lambda$  is larger. The value of  $\xi$  for which this maximum is reached depends slightly on  $\lambda$ , varying nonmonotonically from roughly 0.4 for  $\lambda = 2$  up to 0.2 for  $\lambda = 10$ .

We have compared the result given by this model with existing experimental data and numerical results for various values of  $\lambda$  (Fig. 5). Solid lines correspond to the results given by the model, open symbols to experimental data collected from the works of McGeary (1961), Yerazunis *et al.* (1965), Ben Aïm and Le Goff (1967), and Ridgway and Tarbuck (1968), and filled symbols to numerical simulations made by Rodriguez *et al.* (1986) and Clarke and Wiley (1987). It is well known that experiments are difficult to perform since a size segregation occurs (e.g., the so-called Brazil nuts effect) when the packing is vibrated [Jullien *et al.* (1992)]; hence, a dense packing both random and homogeneous is difficult to obtain. On the other hand, numerical simulations are not so numerous due to large computing time when the size ratio  $\lambda$  is large (the number ratio of the small to large particles increases as  $\lambda^3$ ). Note that segregation can occur with a large aspect ratio in numerical simulations, too. In their simulations for  $\lambda = 5$ , Rodriguez *et al.* (1992) have artificially limited the rolling of the small particles (it takes into account the effects of friction) to avoid this effect.

Note that all these experimental and simulation results do not lead exactly to the value  $c_0 = 0.64$  for the monodisperse packing fraction. However, for the purpose of comparison, we have scaled all the result with this value in Fig. 5. The agreement between the



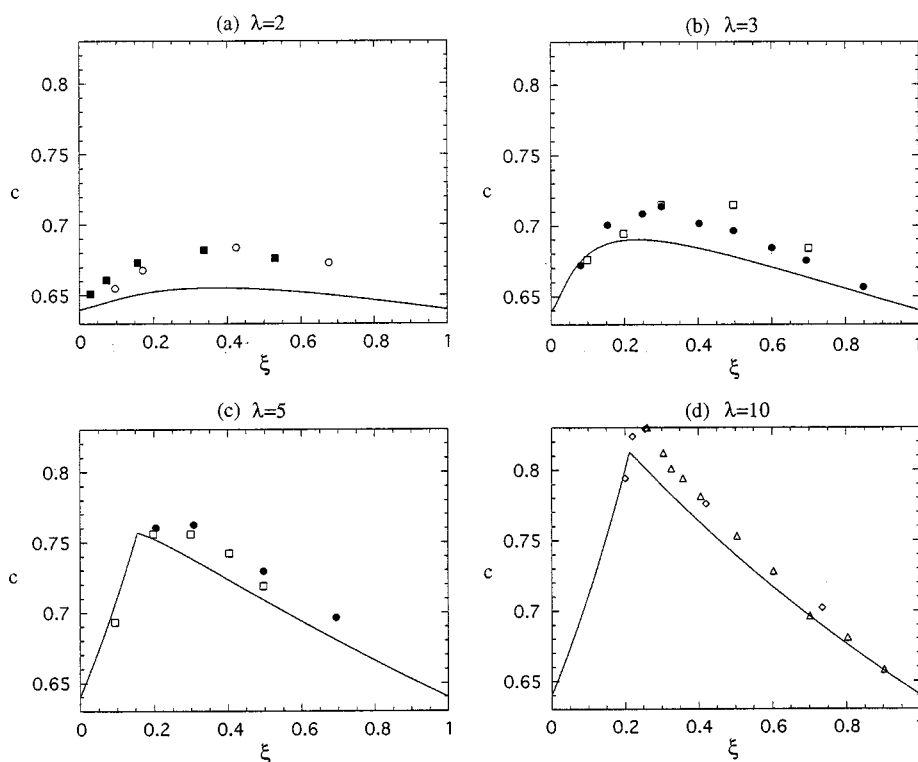


**FIG. 5.** Packing fraction  $c$  of packings of bidisperse spheres as a function of the fraction  $\xi$  of small spheres for size ratio  $\lambda = 2$  (a),  $\lambda = 3$  (b),  $\lambda = 5$  (c), and  $\lambda = 10$  (d). Comparison of the values given by the model (solid line) with experimental data (open symbols) and simulation results (filled symbols). Experimental data are collected from the works of Ridgway and Tarbuck (1968) ( $\circ$ ) for  $\lambda = 2.04$  (a), McGeary (1961) ( $\square$ ) for  $\lambda = 3.45$  (b) and  $\lambda = 4.76$  (c), Ben Aïm and Le Goff (1967) ( $\diamond$ ) for  $\lambda = 8.7$  (d), and Yerazunis *et al.* (1965) ( $\triangle$ ) for  $\lambda = 12$  (d). Simulation results are collected from Clarke and Wiley (1987) ( $\blacksquare$ ) for  $\lambda = 2$  (a) and from Rodriguez *et al.* (1986) ( $\bullet$ ) for  $\lambda = 3$  (b) and  $\lambda = 5$  (c).

model and the data is rather good, in particular for larger values of the size ratio  $\lambda$ . However, for a small size ratio [see Fig. 5(a) for  $\lambda = 2$ ], the model seems to underestimate the increase of the packing fraction upon mixing when compared to experimental and simulation results.

In the following, we present our experimental result for the viscosity measurements of bidisperse suspensions and compare them with the values obtained from the effective medium model described above and with recent simulation results.

### C. Viscosity measurement results

Our results for the dynamic viscosity measurements of bimodal suspension are presented in Fig. 6 (open symbols) as a function of the fraction  $\xi$  of small spheres for different values of the size ratio:  $\lambda = 2$  (a),  $\lambda = 3$  (b),  $\lambda = 5$  (c), and  $\lambda = 10$  (d), and for different values of the total solid volume fraction:  $\Phi = 0.3$  ( $\circ$ ),  $\Phi = 0.4$  ( $\triangle$ ), and  $\Phi = 0.5$  ( $\square$ ). We do not observe, with the precision of our setup, a viscosity decrease upon mixing for the smallest total solid volume fraction  $\Phi = 0.3$ , whatever the size ratio. For larger total solid volume fractions ( $\Phi = 0.4$  and  $\Phi = 0.5$ ), we observe this decrease. Surprisingly, the viscosity decrease upon mixing is not clearly enhanced as the size ratio

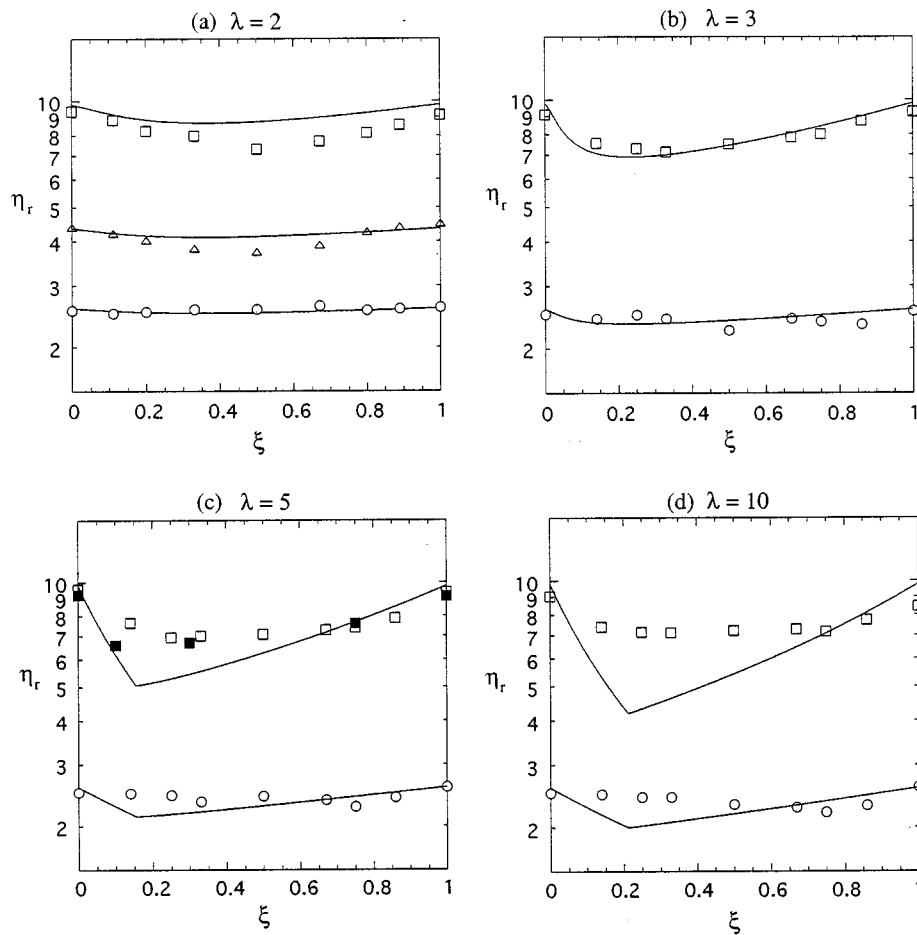


**FIG. 6.** Relative viscosity,  $\eta_r$ , of bidisperse suspensions of spheres as a function of the fraction  $\xi$  of small spheres for size ratio  $\lambda = 2$  (a),  $\lambda = 3$  (b),  $\lambda = 5$  (c), and  $\lambda = 10$  (d). Comparison of the values given by the effective medium model (solid line) with our experimental data (open symbols) and those from Poslinski *et al.* (1988) for a size ratio  $\lambda = 5.3$  (filled symbols) for different total solid volume fractions  $\Phi$  [ $\Phi = 0.3$  (○),  $\Phi = 0.4$  (△), and  $\Phi = 0.5$  (□, ■)].

is increased. For the purpose of comparison, we have also reported the experimental results obtained by Poslinski *et al.* (1988) for the size ratio  $\lambda = 5$  [filled symbols in Fig. 6(c)] with a parallel-plate viscometer and similar systems: bidisperse suspensions of glass spheres ( $d = 15$  and  $80 \mu\text{m}$ ) in a high viscous polymer (polybutene,  $\eta = 25 \text{ Pa s}$ ). Even if these last authors have not reported the dynamic viscosity at a precise frequency but only around a frequency of 10 Hz (they average the measurement over the range 1.6–16 Hz), their values are close to ours.

The variations of the relative viscosity obtained from the effective medium model [Eq. (2)] using for  $\Phi_m(\lambda, \xi)$ , the results obtained from the packing fraction model of Ouchiya and Tanaka (1981), are also presented in Fig. 6 (solid lines). The agreement with the experimental data is rather good for moderate value of the size ratio ( $\lambda = 2$  and 3), meaning that the model we propose catches the essential of the viscosity decrease when particles of different sizes are mixed together. For the smallest size ratio [see Fig. 6(a),

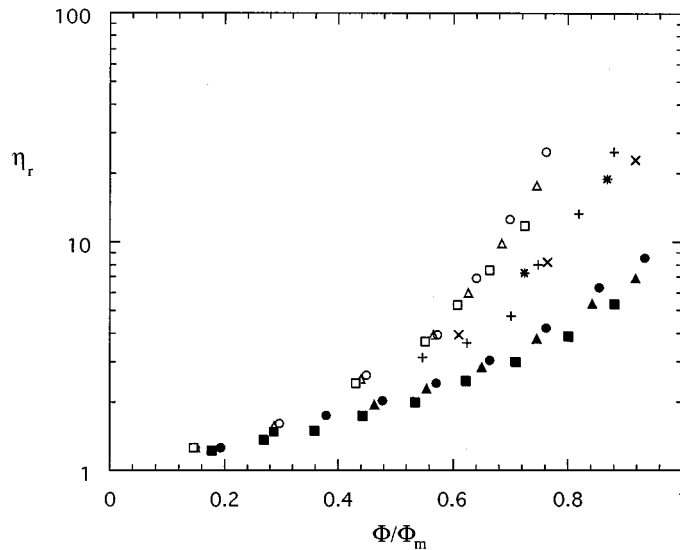


**FIG. 7.** Relative viscosity,  $\eta_r$ , of bidisperse suspensions of spheres as a function of the normalized total solid volume fraction  $\Phi/\Phi_m$  for different size ratio  $\lambda$ . Comparison of our experimental data (crossed symbols) for  $\xi = 0.25$  and  $\lambda = 1$  (+),  $\lambda = 2$  ( $\times$ ), and  $\lambda = 3$  (\*) with the numerical results of Chang and Powell (1994a) by two different techniques: dynamic simulations (open symbols) and Monte Carlo simulations (filled symbols) for  $\xi = 0.27$  and  $\lambda = 1$  (○, ●),  $\lambda = 2$  (△, ▲), and  $\lambda = 4$  (□, ■). The experimental data are normalized by 3D maximum volume fraction and the 2D simulations by 2D maximum volume fraction.

$\lambda = 2$ ], the model underestimates the viscosity decrease upon mixing, but this is due to the fact underlined above that the packing fraction model underestimates the increase of the packing fraction upon mixing at a small size ratio [see Fig. 5(a),  $\lambda = 2$ ]. For the largest value of the size ratio [see Fig. 6(d),  $\lambda = 10$ ], we observe a rather large deviation between the viscosity model and the viscosity measurements. This deviation cannot be attributed to the packing fraction model since it predicts well the packing fraction [see Fig. 5(d),  $\lambda = 10$ ]. The packing fraction might not be the sole parameter that governs the viscosity of bimodal suspensions. The reason for this deviation could possibly be found in the dynamic feature of the flow the suspension is submitted to. Indeed, this feature is not taken into account in the present static description with an effective medium model that involves the packing fraction only. However, note that other experimental data for the viscosity of bidisperse suspensions in steady-shear flows seems to be predicted well by only a packing description [see Probst *et al.* (1994)].

In order to present results concerning different size ratio, we have scaled our experimental data by normalizing the total volume fraction  $\Phi$  by the packing fraction  $\Phi_m(\lambda, \xi)$  given by the model of Ouchiyama and Tanaka (1981) described above. The plot of  $\eta_r$  as a function of  $\Phi/\Phi_m$  for  $\xi = 0.25$  is presented in Fig. 7 [crossed symbols:  $\lambda = 1$  (+),  $\lambda = 2$  ( $\times$ ), and  $\lambda = 3$  (\*)]. All the experimental points fall onto an individual master curve. For the purpose of comparison, the results of the numerical simulations of Chang and Powell (1993, 1994a) for  $\xi = 0.27$  and for the different size ratio are presented in Fig. 7. Note that the scaling with  $\Phi_m(\lambda, \xi)$  ensures that the comparison can be made for any value of  $\lambda$  and  $\xi$ . However, as Chang and Powell (1994a, 1994b), we have chosen one value of  $\xi$  in order to keep Fig. 7 as clear as possible. In Fig. 7, the plain symbols correspond to the Monte Carlo technique and the open ones to the dynamic simulations. For these two simulations, which are two-dimensional ones, the solid area fraction has

been normalized by the two-dimensional packing fraction [see Fig. 6 of Chang and Powell (1994a)]. With the Monte Carlo technique, the microstructure of the suspension is frozen and leads to the viscosity at infinite frequency. On the other hand, with dynamic simulation, the suspension microstructure evolves at each step and leads to the viscosity at zero frequency. Dynamic simulations yield higher viscosities as compared with the results of Monte Carlo simulations. Our experimental results, which correspond to the finite-frequency case, lead to intermediate values between the two different kinds of simulations. Such a viscosity decrease when increasing the shear frequency is observed in Brownian suspensions [Bossis and Brady (1989), Van der Werff and De Kruif (1989)], as well as in non-Brownian ones [Poslinski *et al.* (1988), Gondret *et al.* (1996)]. If this phenomenon is well known and well understood for the Brownian suspensions, the control parameter being the Péclet number, this is not the case, however, for the non-Brownian ones.

#### IV. CONCLUSION

In this paper, we have reported experimental results for the viscosity measurement at finite frequency, which show a decrease in the dynamic viscosity of bidisperse macroscopic suspensions when one mixes particles of two sizes. On the one hand, we have interpreted these results from the influence of the size distribution of the particle mixture (characterized by the size ratio and the fraction of small spheres to the total solids) on the packing fraction and, consequently, on the viscosity of the suspensions. On the other hand, we have compared our results with numerical simulations performed by Stokesian dynamics and Monte Carlo technique. Our measurement obtained at finite frequency lead to intermediate values between those obtained by the two types of simulations and corresponding to the viscosity at zero and infinite frequency, respectively.

#### ACKNOWLEDGMENTS

This work has been supported by the Centre National d'Études Spatiales under a grant (No. 93/CNES/0391) and has been made in the frame of the Groupement De Recherches "Physique des Milieux Hétérogènes Complexes" of the Centre National de la Recherche Scientifique (CNRS). The experiments have been performed in the Laboratoire de Physique de l'École Normale Supérieure de Lyon. The authors gratefully acknowledge Georges Bossis for fruitful discussions on the subject.

#### References

- Ball, R. C. and P. Richmond, "Dynamics of colloidal dispersions," *Phys. Chem Liq.* **9**, 99–116 (1980).
- Ben Aim, R. and P. Le Goff, "Effet de paroi dans les empilements désordonnés de sphères et application à la porosité de mélange binaires," *Powder Technol.* **1**, 281–290 (1967).
- Bossis, G. and J. F. Brady, "The rheology of Brownian suspensions," *J. Chem. Phys.* **91**, 1866–1874 (1989).
- Brady, J. F., "The rheological behavior of concentrated colloidal dispersions," *J. Chem. Phys.* **99**, 567–581 (1993).
- Chang, C. and R. L. Powell, "Dynamic simulation of bimodal suspensions of hydrodynamically interacting spherical particles," *J. Fluid Mech.* **253**, 1–25 (1993).
- Chang, C. and R. L. Powell, "The rheology of bimodal hard-sphere dispersions," *Phys. Fluids* **6**, 1628–1636 (1994a).
- Chang, C. and R. L. Powell, "Effect of particle size distribution on the rheology of concentrated bimodal suspensions," *J. Rheol.* **38**, 85–98 (1994b).
- Cheng, D. C.-H., P. Kruszewski, J. R. Senior, and T. A. Roberts, "The effect of particle size distribution on the rheology of an industrial suspension," *J. Mater. Sci.* **25**, 353–373 (1990).

- Chong, J. S., E. B. Christiansen, and A. D. Baer, "Rheology of concentrated suspensions," *J. Appl. Polym. Sci.* **15**, 2007–2021 (1971).
- Clarke, A. S., and J. D. Wiley, "Numerical simulation of the dense random packing of a binary mixture of hard spheres: Amorphous metals," *Phys. Rev. B* **35**, 7351–7356 (1987).
- D'Haene, P. and J. Mewis, "Rheological characterization of bimodal colloidal dispersions," *Rheol. Acta* **33**, 165–174 (1994).
- De Kruif, C. G., E. M. F. Van Iersel, A. Vrij, and W. B. Russel, "Hard sphere colloidal dispersions: Viscosity as function of shear rate and volume fraction," *J. Chem. Phys.* **83**, 4717–4725 (1985).
- Dodds, J. A., "The porosity and contact points in multicomponent random sphere packings calculated by a simple statistical geometric model," *J. Colloid Interface Sci.* **77**, 317–327 (1980).
- Eveson, G. F., "The viscosity of stable suspensions of spheres at low rates of shear," *Rheology of Disperse Systems* (Pergamon, New York, 1959), pp. 61–83.
- Farris, R. J., "Prediction of the viscosity of multimodal suspensions from unimodal viscosity data," *Trans. Soc. Rheol.* **12**, 281–301 (1968).
- Gondret, P. and L. Petit, "Crystallisation of macroscopic suspensions under shear: Influence of particle size distribution," *Europhys. Lett.* **22**, 347–352 (1993).
- Gondret, P. and L. Petit, "Viscosity of disordered and ordered suspensions of solid spheres: Experimental results and models," *C. R. Acad. Sci., Ser. IIB: Mec. Phys., Chim., Sci. Terre Univers* **321**, 25–31 (1995).
- Gondret, P. and L. Petit, "Viscosity of periodic suspensions," *Phys. Fluids* **8**, 2284–2290 (1996).
- Gondret, P., L. Petit, and G. Bossis, "Static and dynamic viscosity of macroscopic suspensions of solid spheres," *Proceedings of the XIIth International Congress on Rheology*, edited by A. Ait-Kadi, J. M. Dealy, D. F. James, and M. C. Williams, August 13–23, Quebec City (Quebec), Canada (1996).
- Goto, H. and H. Kuno, "Flow of suspensions containing particles of two different sizes through capillary tubes," *J. Rheol.* **26**, 387–398 (1982).
- Goto, H. and H. Kuno, "Flow of suspensions containing particles of two different sizes through capillary tubes. 2-Effects of the particle size ratio," *J. Rheol.* **28**, 197–205 (1984).
- Gupta, R. K. and S. G. Seshadri, "Maximum loading levels in filled liquid systems," *J. Rheol.* **30**, 503–508 (1986).
- Hoffman, R. L., "Factors affecting the viscosity of unimodal and multimodal colloidal dispersions," *J. Rheol.* **36**, 947–965 (1992).
- Jeffrey, D. J., "The calculation of low Reynolds number resistance functions for two unequal spheres," *Phys. Fluids A* **4**, 16–29 (1992).
- Jullien, R., P. Meakin, and A. Pavlovitch, "Three-dimensional model for particle-size segregation by shaking," *Phys. Rev. Lett.* **69**, 640–646 (1992).
- Kim, I. T. and P. F. Luckham, "Some rheological properties of bimodal sized particulates," *Powder Technol.* **77**, 31–37 (1993).
- Lee, D. I., "Packing of spheres and its effects on the viscosity of suspensions," *J. Paint Technol.* **42**, 579–587 (1970).
- McGeary, R. K., "Mechanical packing of spherical particles," *J. Am. Ceram. Soc.* **44**, 513–522 (1961).
- Miller, R. R., E. Lee, and R. L. Powell, "Rheology of solid propellant dispersions," *J. Rheol.* **35**, 901–920 (1991).
- Nolan, G. T. and P. E. Kavanagh, "Computer simulation of random packings of hard spheres," *Powder Technol.* **72**, 149–155 (1992).
- Ouchiya, N. and T. Tanaka, "Porosity of a mass of solid particles having a range of sizes," *Ind. Eng. Chem. Fundam.* **20**, 66–71 (1981).
- Parkinson, C., S. Matsumoto, and P. Sherman, "The influence of particle-size distribution on the apparent of non-Newtonian dispersed systems," *J. Colloid Interface Sci.* **33**, 150–160 (1970).
- Petit, L. and P. Gondret, "Self-diffusion of particles in an alternatively sheared macroscopic suspension," *J. Phys. II (France)* **3**, 301–307 (1993).
- Poslinski, A. J., M. E. Ryan, R. K. Gupta, S. G. Seshadri, and F. J. Frechette, "Rheological behaviour of filled polymeric systems. 2-The effect of a bimodal size distribution of particulates," *J. Rheol.* **32**, 751–771 (1988).
- Probstein, R. F., M. Z. Sengun, and T.-C. Tseng, "Bimodal model of concentrated suspension viscosity for distributed particle sizes," *J. Rheol.* **38**, 811–829 (1994).
- Ridgway, K. and K. J. Tarbuck, "Particulate mixture bulk densities," *Chem. Process. Eng.* **49**, 103–105 (1968).
- Rodriguez, B. E., E. W. Kaler, and M. S. Wolfe, "Binary mixtures of monodisperse latex dispersions. 2. Viscosity," *Langmuir* **8**, 2382–2389 (1992).
- Rodriguez, J., C. H. Allibert, and J. M. Chaix, "A computer method for random packing of spheres of unequal size," *Powder Technol.* **47**, 25–33 (1986).
- Sadoc, J.-F., "Calcul de la densité maximale d'un empilement aléatoire de sphères dures identiques," *C. R. Acad. Sci. Paris Ser. II: Mec. Phys., Chim., Sci. Terre Univers*, **292**, 435–438 (1981).

- Scott, G. D. and D. M. Kilgour, "The density of random close packing of spheres," *Brit. J. Appl. Phys. (J. Phys.)* **2**, 863–866 (1969).
- Shapiro, A. P. and R. F. Probst, "Random packings of spheres and fluidity limits of monodisperse and bidisperse suspensions," *Phys. Rev. Lett.* **68**, 1422–1425 (1992).
- Sengun, M. Z. and R. F. Probst, "Bimodal model of slurry viscosity with application to coal-slurries. Part 1. Theory and experiment," *Rheol. Acta* **28**, 382–393 (1989).
- Storms, R. F., B. V. Ramarao, and R. H. Weiland, "Low shear viscosity of bimodally dispersed suspensions," *Powder Technol.* **63**, 247–259 (1990).
- Sweeny, K. H. and R. D. Geckler, "The rheology of suspensions," *J. Appl. Phys.* **25**, 1135–1144 (1954).
- Van de Ven, T. G. M., *Colloidal Hydrodynamics* (Academic, London, 1989).
- Van der Werff, J. C. and C. G. De Kruif, "Hard-sphere colloidal dispersions: The scaling of rheological properties with particle size, volume fraction, and shear rate," *J. Rheol.* **33**, 421–454 (1989).
- Wagner, N. J. and A. T. J. Woutersen, "The viscosity of bimodal and polydisperse suspensions of hard spheres in the dilute limit," *J. Fluid Mech.* **278**, 267–287 (1994).
- Woutersen, A. T. J. M. and C. G. De Kruif, "The viscosity of semidilute, bidisperse suspensions of hard spheres," *J. Rheol.* **37**, 681–693 (1993).
- Yerazunis, S., S. W. Cornell, and B. Wintner, "Dense random packing of binary mixtures of spheres," *Nature (London)* **207**, 835–837 (1965).